ELSEVIER

Journal of Biomechanics 39 (2006) 1964–1982

JOURNAL OF BIOMECHANICS

www.elsevier.com/locate/jbiomech
www.JBiomech.com

Numerical simulation of cardiovascular dynamics with healthy and diseased heart valves

Theodosios Korakianitis*, Yubing Shi

Department of Mechanical Engineering, University of Glasgow, Glasgow G12 8QQ, UK

Accepted 27 June 2005

Abstract

This paper presents a new concentrated parameter model for cardiovascular dynamics that includes an innovative model of heart valve dynamics, which is embedded in the overall model of the four chambers of the heart and the systemic and pulmonary circulation loops. The heart chambers are described with a variable elastance model, and the systemic and pulmonary loops are described with modified Windkessel models. In modelling the heart valve dynamics, the various factors that influence the valve motion are examined, and the governing differential equation for valve motion is derived. The heart valve model includes the influence of the blood pressure effect, the friction effect from the tissue, and from blood motion. As improvement from previous works, the contribution of the blood vortex effect in the vicinity of the valve leaflets to valve motion is specially considered. The proposed model is then used in simulation of healthy and certain pathological conditions such as mitral valve stenosis and aortic regurgitation. The predicted results agree well with results illustrated in cardiology textbooks.

Keywords: Numerical simulation; Cardiovascular dynamics; Heart valve model; Stenosis; Regurgitation

1. Introduction

As important accessories to the heart, the mitral, aortic, tricuspid and pulmonary valves function to keep the one way flow direction in the cardiovascular system. Normal function of the 4 valves has a great impact on the pathophysiological processes in the cardiovascular system. Thus, analysis of flow dynamics in heart valves is an active research area.

In a typical heart cycle, blood flows from the left and right atria to the corresponding ventricles in diastole. The mitral/tricuspid valves are open and the aortic and pulmonary valves are closed. At the end of diastole, the mitral/tricuspid valves close. Then systole starts and the ventricles enter the iso-volumic contraction phase. Next the aortic/pulmonary valves open, and the heart enters peak systolic phase. At the end of systole the aortic/pulmonary valves close, and the iso-volumic relaxation phase begins in the ventricles. Next the mitral/tricuspid valves open and the heart begins the diastolic phase. This apparently simple cyclic process presents unexpected fluid dynamic complexities in the details. The exact mechanism of heart valve motion has puzzled researchers for decades. Several assumptions have been proposed to explain valve motion dynamics. In explaining valve motion Leonardo da Vinci used the aortic valve as example, and proposed that the vortex formed in the sinus of Valsalva is the driving force for valve motion (Fung, 1984). Today most researchers think that the pressure difference across the valve is the dominant factor for valve motion. The arguments are still ongoing and no authoritative conclusion has been reached yet.

To clarify this simple yet complex valve motion mechanism, extensive numerical and experimental studies have been carried out. Most experimental studies were based on in vitro observations with

*Corresponding author. Tel.: +44 141 330 2490; fax: +44 141 330 2480.
E-mail address: t.alexander@mech.gla.ac.uk (T. Korakianitis).

0021-9290/$ - see front matter © 2004 Elsevier Ltd. All rights reserved.
doi:10.1016/j.jbiomech.2005.06.016

Nomenclature

A	sectional area
C	compliance
CQ	flow coefficient
DT	Time step
E	elastance
I	inertial moment of rotating
K, k	coefficient
L	inertance
M	mass
P	pressure
Q	flow rate
R	resistance
T	time; heart period
V	volume
θ	rotating angle of valve leaflet

Subscripts

0	initial value; offset value; value for unstressed condition
ao	aortic valve
bm	velocity effect on the valve dynamics, due to blood motion
d	diastolic phase
e	elastance action
ea	elastance of atrium
ev	elastance of ventricle
f	frictional action
fr	frictional effect on the valve dynamics, due to resistance of neighboring tissue
la	left atrium
lv	left ventricle
max	maximum value
min	minimum value
mi	mitral valve
p	effect of pressure force
par	pulmonary arterioles
pas	pulmonary aortic sinus
pat	pulmonary artery
pav	right annulus fibrosus
pcp	pulmonary capillary
po	pulmonary aortic valve
pr	pressure effect on the valve dynamics
pvc	pulmonary venae cavae
pvn	pulmonary vein
pwb	beginning of P wave
pww	duration of P wave
ra	right atrium
rv	right ventricle
s	systolic phase
s1	peak of systolic phase
s2	end of systolic phase
sar	systemic arterioles
sas	systemic aortic sinus
sat	systemic artery
sav	left annulus fibrosus
scp	systemic capillary
ss	effect of shear stress on the valve dynamics
st	strain action
svc	systemic venae cavae
svn	systemic vein
ti	tricuspid valve
vo	vortex effect on the valve dynamics

echo-cardiography (Chambers and Ely, 1998; Durand et al., 1999), particle image velocimetry (PIV) (Brucker, 1997; Lim et al., 1998; Subramanian Mu et al., 2000), laser Doppler velocimetry (LDV) (Chew et al., 1993; Grigioni et al., 2000), or with hot wire probes (Healy et al., 1998). These studies emphasized other aspects of fluid flow in the valve, while the sinus of Valsalva were often simplified or eliminated in the test rig design. Thus, the flow field was distorted and the effect of the blood-flow vortex around the valves was not well represented. To compensate for this shortcoming, several clinical observations have been conducted. Leyh et al. (1999) conducted transthoracic and transesophageal echo-cardiographic studies on 20 human subjects experiencing different valve-sparing surgery techniques on aortic valves, and found that the aortic valve undergoes a three-stage motion pattern: a rapid early systolic opening, a slow middle systolic closing, and a rapid early diastolic closing movement. Besides the three-stage motion pattern, published clinical observations also revealed that in the mitral valves, there is a regression motion for the leaflet to return to the fully open position before the rapid early diastolic closing (Berne and Levy, 1981; Levick, 2003). To further explore the valve motion mechanism, Yacoub et al. (1996) obtained photomicrographs of interstitial cells cultured from human aortic valve, and measured the tissue motion and blood motion around the aortic valve with transesophageal echo cardiography and MRI technique. Based on results of observation and measurements, Yacoub et al. extended Leonardo da Vinci's idea and suggested that aortic flow is a tale of dynamism and crosstalk between the blood and the surrounding structures including the sinuses of Valsalva, valve cusps, and the contracting ventricle chamber. Besides the contraction motion of the ventricle chamber, the aortic root and valve cusps also have smooth muscles that contribute to the crosstalk. In this complex interaction,

the vortices formed in the sinuses of Valsalva play an important role in keeping smooth valve opening and closure and maintaining coronary flow. Among all the descriptions of valve motion, this opinion gives the most detailed and in-depth description of the physiological phenomena in aortic flow.

Previous research in numerical study of blood flow in heart valves can be categorized into two groups: concentrated parameter studies and distributed parameter studies. Concentrated parameter studies focus on global analysis of cardiovascular dynamics, in which heart valve dynamics is only part of the model, and the valve is modelled with a very simple description. Among them, most of earlier researchers modelled the heart valve as a diode plus a linear or nonlinear resistance (Drzewiecki et al., 1996; Heldt et al., 2002; Pennati et al., 1997; Vollkron et al., 2002). This description puts more emphasis on the ideal characteristic of the one way flow direction in the heart valve, while the more complex feature of valve dynamics was ignored, so that local hemodynamics in valves such as the regurgitant (reverse) flow were not simulated. Recent research has noted this deficiency and developed more realistic and complex valve behavior models. Žáček and Krause (1996) considered the change of heart valve resistance during valve motion by using the concept of time-dependent drag coefficient. In their work the drag coefficient was a prescribed function of the valve open area, and it approached infinity when the valve was closed. The drag coefficients were added to the losses of the conduit where the valve was situated. Werner et al. (2002) described the valve behavior by considering the volume of the reverse flow in the valve upon valve closure, which was prescribed in their study and was called the dead space volume. The dead space volume was a function of the valve leaflet opening angle, and it became zero when the valve was fully closed. Shi et al. (2004) modelled the valve dynamics by considering the local flow resistance and the blood inertial effect. The valve was described with an orifice model, and the valve opening change was prescribed based on previous experimental observations. These three models improved heart valve modelling. However, in all these models the valve behavior was prescribed, while the underlying valve dynamics and motion mechanism were not considered. As an alternative, in distributed parameter studies the emphasis is mostly on local flow field features in the heart valve. These studies usually involve computational fluid dynamics (CFD) to calculate the pressure and velocity distribution in a two-dimensional or three-dimensional flow field configuration around the heart valves, with artificial boundary conditions set upstream and downstream. This kind of computation always requires expensive computing resources. As heart valve diseases usually occur in the systemic circulation, the aortic and mitral valves are predominantly the targets of research. Many computational studies concentrate on artificial heart valves, due to their simple geometry and motion trajectory. Due to limitation of computing facilities, early research of this kind concentrated on the steady or unsteady flow in aortic and mitral valves in peak systolic phase (Bluestein and Einav, 1994; Huang et al., 1994; Shim and Chang, 1997; Underwood, 1975). As more powerful computers became available, some researchers began to target modelling the moving valve leaflet and blood–leaflet interaction (Kiris et al., 1997; Makhijani et al., 1996a,b, 1997; Shi et al., 2003; De Hart et al., 2000, 2003a, 2003b; Lai et al., 2002).Limitations in computing resources and numerical methods greatly restricted these attempts. Realistic modelling of valve motion dynamics can only be carried out with considerable simplifications in these computational studies, e.g., omitting the contraction and elasticity of the valve cusps and aortic root, ignoring the vortices effect in the sinuses of Valsalva, and considering only the effect of pressure difference and shear stress in the valve.

The current paper balances the above two ways of numerical analysis, thus increasing the modelling accuracy of valve dynamics with affordable computational expense. The valve is considered as a concentrated parameter component, and the governing differential equation for valve dynamics is derived by considering the various forces acting on the valve. The developed valve model is then coupled with the concentrated parameter description of the whole cardiovascular system. Compared to previous research, this new valve model greatly improves the simulation results. The new valve model is used to study the cardiac flow in certain healthy and diseased heart valves, and the simulation provides comparable results to those illustrated in medical textbooks.

2. Method

2.1. Mathematical model

A schematic of the whole circulation system is provided in Fig. 1. The system is modelled in three main parts: heart, systemic circulation loop, and pulmonary circulation loop. The heart is modelled as four chambers with variable or constant elastance and four heart valves that control the blood flow direction. The systemic and pulmonary circulation loops are each separated into aortic sinus, artery, arteriole, capillary, and vein segments. In every segment the individual component is modelled by considering the local resistance to blood flow, elasticity of blood vessels, and inertia of blood. The artery segment represents the general characteristics of both the aorta and smaller arteries in the present work. The aortic sinus is specially separated from the artery modelling for easy estimation

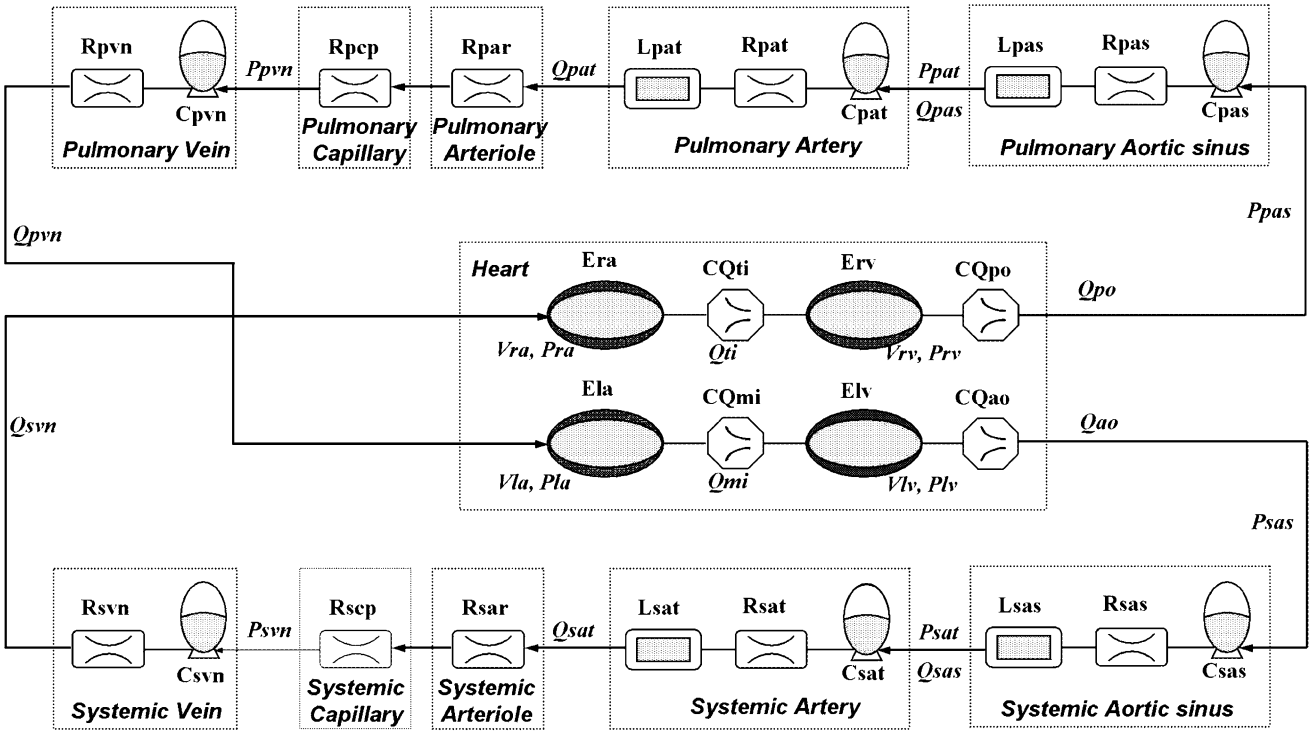

Fig. 1. Schematic of the circulation system model.

of pressure response in the aortic arch, to facilitate future inclusion of the autonomic regulation mechanism. The combined effect of venule, vein, and vena cava is modelled as the vein segment.

2.1.1. Heart chambers

In modelling the heart, the basic ventricle function is described with the pressure–volume relation using Suga et al's, (1975) variable elastance model. In the left ventricle, the volume change is derived by the flow difference between mitral and aortic valves:

$$\frac{dV_{lv}}{dt} = Q_{mi} - Q_{ao}. \tag{1}$$

The time-varying left ventricular elastance, illustrated in Fig. 2, is a function of the characteristic elastance ($E_{lv,s}$ and $E_{lv,d}$) and an activation function $e(t)$:

$$e_{lv}(t) = E_{lv,d} + \frac{E_{lv,s} - E_{lv,d}}{2} e(t). \tag{2}$$

A commonly used ventricular activation function is used in the current work:

$$e(t) = \begin{cases} \cos\left(\dfrac{t}{T_{s1}}\pi\right), & 0 \leqslant t < T_{s1}, \\ \cos\left(\dfrac{t + T_{s2} - T_{s1}}{T_{s1}}\pi\right), & T_{s1} \leqslant t < T_{s2}, \\ 0, & T_{s2} \leqslant t < T. \end{cases} \tag{3}$$

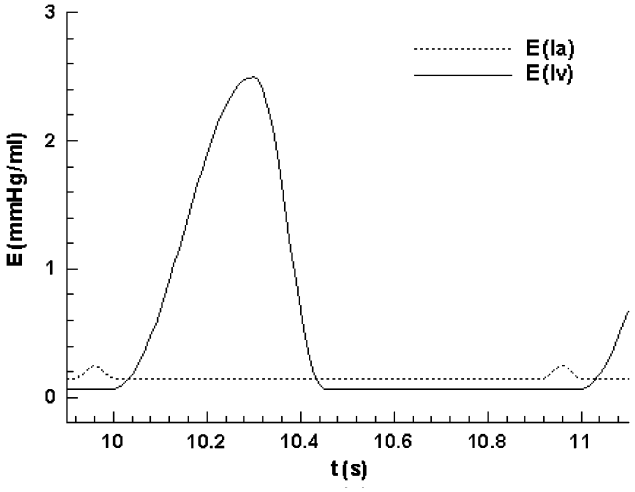

Fig. 2. Elasticity changes in the left ventricle and the left atrium under normal operation.

The pressure in the left ventricle is then derived from the instantaneous volume and elastance values in the ventricle

$$P_{lv} = P_{lv,0} + e_{lv}(V_{lv} - V_{lv,0}). \tag{4}$$

Modelling of the right ventricle is similar to the above process, with detailed parameters changed. Modelling of the left and right atria are similar to that for the

ventricles, but with different activation function for the elastance change

$$e(t)=\begin{cases}0, & 0\leqslant t<T_{\mathrm{pb}},\\ 1-\cos\left(\dfrac{t-T_{\mathrm{pb}}}{T_{\mathrm{pw}}}2\pi\right), & T_{\mathrm{pb}}\leqslant t<T_{\mathrm{pb}}+T_{\mathrm{pw}},\\ 0, & T_{\mathrm{pb}}+T_{\mathrm{pw}}\leqslant t<T.\end{cases} \tag{5}$$

The elastance change in the left atrium is also illustrated in Fig. 2.

2.1.2. Heart valve

Most prior studies have modelled heart valves as resistance components in the fully open or fully closed situation, while the opening and closing processes were not considered. There were some who considered the opening and closing processes, such as Žáček and Krause (1996); Werner et al. (2002), and Shi et al. (2004), but they used prescribed functions to describe the valve behavior, while the valve dynamics and motion mechanism were not analyzed. In the current model, the basic pressure–flow relation in the aortic valve is described with an orifice model

$$Q_{\mathrm{ao}}=\begin{cases}CQ_{\mathrm{ao}}\cdot AR_{\mathrm{ao}}\cdot\sqrt{P_{\mathrm{lv}}-P_{\mathrm{sas}}}, & P_{\mathrm{lv}}\geqslant P_{\mathrm{sas}},\\ CQ_{\mathrm{ao}}\cdot AR_{\mathrm{ao}}\cdot\sqrt{P_{\mathrm{sas}}-P_{\mathrm{lv}}}, & P_{\mathrm{lv}}<P_{\mathrm{sas}},\end{cases} \tag{6}$$

while the valve opening AR_{ao} is derived in two ways. In the first, simplified model, like that in most prior studies, the valve opening switches between 0 and 1 corresponding to fully closed and fully open positions, depending on which side of valve has a higher pressure:

$$AR_{\mathrm{ao}}=\begin{cases}1, & P_{\mathrm{lv}}\geqslant P_{\mathrm{sas}},\\ 0, & P_{\mathrm{lv}}<P_{\mathrm{sas}}.\end{cases} \tag{7}$$

In the newly developed model in the current research, the valve motion mechanism is analyzed by considering the blood–valve interaction effect. The valve opening is decided by the angular position of the valve leaflets:

$$AR_{\mathrm{ao}}=\frac{A_{\mathrm{ao}}(1-\cos\theta)^2}{A_{\mathrm{ao}}(1-\cos\theta_{\max})^2}=\frac{(1-\cos\theta)^2}{(1-\cos\theta_{\max})^2}, \tag{8}$$

while the leaflet angular position is computed by considering the various factors that affect the leaflet motion. These include the blood-flow effects of: pressure difference across the valve; the frictional effect from neighboring tissue resistance; the dynamic motion effect of the blood acting on the leaflet; the action of the vortex downstream of the valve; and shear stress on the leaflet. Thus, the external forces acting on the leaflet are illustrated in Fig. 3. The valve motion is governed by

$$I_{\mathrm{ao}}\frac{\mathrm{d}^2\theta}{\mathrm{d}t^2}=F_{\mathrm{pr}}-F_{\mathrm{fr}}+F_{\mathrm{bm}}-F_{\mathrm{vo}}+F_{\mathrm{ss}}. \tag{9}$$

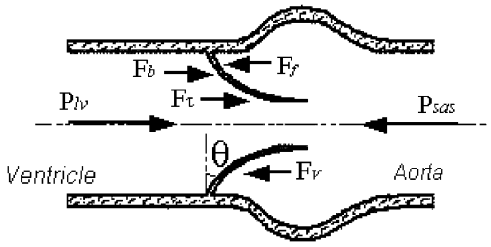

Fig. 3. Illustration of typical forces acting on a heart valve leaflet.

Here the pressure effect is represented to be proportional to normal component of the pressure effect on the valve leaflet surface:

$$F_{\mathrm{pr}}=(P_{\mathrm{lv}}-P_{\mathrm{sas}})k_{\mathrm{p,ao}}\cos\theta. \tag{10}$$

The frictional effect due to resistance in the tissue at valve root is assumed to be proportional to the leaflet angular velocity

$$F_{\mathrm{fr}}=k_{\mathrm{f,ao}}\frac{\mathrm{d}\theta}{\mathrm{d}t}. \tag{11}$$

The fluid velocity effect is modelled as proportional to the flow rate normal to the leaflet surface

$$F_{\mathrm{bm}}=k_{\mathrm{b,ao}}Q_{\mathrm{ao}}\cos\theta. \tag{12}$$

Based on the CFD results of Shi et al. (2003) and De Hart et al. (2000, 2003a,b), the shear stress force is very small and is neglected ($F_{\mathrm{ss}}\approx 0$).

The vortex effect on valve motion is the subject of ongoing investigations. Yacoub et al.'s work (Yacoub et al., 1996) strongly suggests that the vortex effect is one of the very important factors that govern valve dynamics. Also according to Bellhouse (1972), neglecting the vortex effect in valve modelling will cause overestimation of the reverse flow during valve closure. Thus, it is very important to include the vortex effect in the valve dynamics modelling. The vortex effect on the valve should be modelled by the local vorticity distribution, which is only possible with the distributed parameter studies using 2D or 3D CFD, and focusing on local flow features. However, even previous 2D (De Hart et al., 2000) or 3D (Shi et al., 2003; De Hart et al., 2003a,b) CFD analysis failed to provide a clear understanding of the vortex effect on valve motion, due to limitations in both the numerical methods and the computing facilities. Thus, for the purposes of this paper, the only remaining method of study is intuitive modelling based on experimental and clinical observations, and subjective understanding of the valve motion physics.

From previous experimental observations (Brucker, 1997; Lim et al., 1998; Subramanian Mu et al., 2000; Chew et al., 1993; Grigioni et al., 2000; Leyh et al.,

1999), it is intuitively understood that the vortex intensity is closely related to the fluid flow rate across the valve and the leaflet angular position. Take the aortic valve for example. In early systole, with the contraction of the left ventricle the forward flow across the aortic valve is ever-increasing as jet flow, the valve is in the opening process, and there are vortices developing in the aortic sinus. This trend lasts until an instance when the valve leaflet opens to, approximately, the valve half-open position. After this instance, the aortic flow is still increasing, and the valve is still in the opening process, but the motion of valve leaflets reduces the allowable space for the vortex in the aortic sinus, so that after the valve half-open position the vortex intensity is decreasing. This situation continues until the valve leaflets reach the fully open position, and the forward aortic flow becomes weak, in late systole. In late systole and early diastole, the aortic flow changes from weak forward flow to weak backward flow. When the backward aortic flow develops, the vortices become merged into the strong backward flow and lose the effect, thus no vortex effect needs to be considered then.

Based on this understanding, a term in the form of the product of the flow rate and the effect of the leaflet angular position is constructed to represent the vortex effect in the heart valve dynamics. It is understood that the bigger the flow rate in the valve, the stronger the vortex intensity near the valve. Also, it is assumed that vortex intensity reaches the maximum value when the leaflet is at about 45° opening angle. Below 45°, the smaller the valve opening angle, the more likely for the flow to pass the valve as jet flow. Similarly, above 45°, the bigger the valve opening angle, the more likely the leaflet will cover the valve root area and restrict the vortex formation. Thus, F_{vo} is given by

$$F_{vo} = \begin{cases} k_{v,ao} Q_{ao} \sin 2\theta, & Q_{ao} \geqslant 0, \\ 0, & Q_{ao} < 0. \end{cases} \tag{13}$$

Combining the above effects and substituting $K = k/I_{ao}$:

$$\frac{d^2\theta}{dt^2} = \begin{cases} = & (P_{lv} - P_{sas}) K_{p,ao} \cos\theta - K_{f,ao} \dfrac{d\theta}{dt} \\ & + K_{b,ao} Q_{ao} \cos\theta - K_{v,ao} Q_{ao} \sin\theta, \quad Q_{ao} \geqslant 0, \\ = & (P_{lv} - P_{sas}) K_{p,ao} \cos\theta - K_{f,ao} \dfrac{d\theta}{dt} \\ & + K_{b,ao} Q_{ao} \cos\theta, \quad Q_{ao} < 0. \end{cases} \tag{14}$$

This detailed consideration of valve dynamics helps to describe the regurgitant flow in the valve, thus improving the accuracy of the simulation. Modelling of the remaining three valves is implemented in a similar way, with different values of parameters in the equations.

2.1.3. Blood circulation loops

In modelling systemic circulation components, depending on detailed local flow conditions, the frictional loss, elastance, and blood inertia are modelled as resistance, compliance, and inductance effects following the classical idea of the electric-fluid analogue. The systemic circulation loop is divided into five parts of aortic sinus, artery, arterioles, capillary, and vein. The aortic sinus and artery are quite elastic, and the flow is pulsatile in these segments, so that all the resistance, compliance, and inductance effects are considered. Arterioles and capillaries are dominated by resistance effects. Vein functions to collect and store blood, thus resistance and compliance effects are considered in the vein model.

Great pressure and flow rate oscillations are experienced in the aortic sinus due to the local tissue elastance and flow variations. The pressure is governed by

$$\frac{dP_{sas}}{dt} = \frac{Q_{ao} - Q_{sas}}{C_{sas}} \tag{15}$$

and the flow rate is:

$$\frac{dQ_{sas}}{dt} = \frac{P_{sas} - P_{sat} - R_{sas} Q_{sas}}{L_{sas}}. \tag{16}$$

The pressure and flow rate changes in the artery are similar to those in the aortic sinus. As arterioles and capillaries are both considered as pure resistance units, their effects are integrated with the artery as resistance units. Thus, the pressure equation is

$$\frac{dP_{sat}}{dt} = \frac{Q_{sas} - Q_{sat}}{C_{sat}} \tag{17}$$

and the flow rate equation is

$$\frac{dQ_{sat}}{dt} = \frac{P_{sas} - P_{svn} - (R_{sat} + R_{sar} + R_{scp}) Q_{sat}}{L_{sat}}. \tag{18}$$

The systemic vein is modelled as a compliance unit combined with a resistance unit. In the vein the pressure is

$$\frac{dP_{svn}}{dt} = \frac{Q_{sat} - Q_{svn}}{C_{svn}} \tag{19}$$

and the flow rate is given by

$$Q_{svn} = \frac{P_{svn} - P_{ra}}{R_{svn}}. \tag{20}$$

The model of the pulmonary loop is similar to that of the systemic loop, with different values for system parameters.

2.2. System parameters

Values for the physiological parameters are usually difficult to measure, and they change from person to person. This is a common problem in medical and biomedical studies. To minimize the potential influence of the values of these parameters on the results, great care was taken to assign values to these physiological variables based on data in widely referred papers and

textbooks. Where no such data were available, great effort was made to find the reasonable range of values for the variables from the open literature.

Most researchers used the variable elastance model to describe the heart dynamics. In the current research chamber elastance values are assigned as shown in Table 1, based on parameter selection in (Ursino, 1999; Lu et al., 2001; Heldt et al., 2002; Thomas et al., 1997). Parameter settings for systemic and pulmonary loops are based on (Ursino, 1999; Lu et al., 2001; Thomas et al., 1997; Ursino, 1998), as shown in Table 2. In modelling heart valve dynamics, coefficients for valve motion equations, shown in Table 3, are selected through numerical experiments to find the optimal parameter combinations that produce near physiological valve motion process as described in the literature (Leyh et al., 1999; Levick, 2003; Shi et al., 2003; De Hart et al., 2003a). Valve opening angles, illustrated in Table 4, are set by reference to physiological textbooks and the parameters of mainstream artificial heart valves. Other parameters such as systolic duration, the beginning instance and duration of the P wave in the ECG signal, the time step of simulation, etc., were chosen based on general knowledge in physiological textbooks (Guyton, 1986; West, 1990). Table 5 shows values for these parameters.

3. Results

Based on the mathematical model described above, a program is developed in C language to simulate the dynamic changes in the cardiovascular system, especially in the heart valve regions. In the study, first the traditional heart valve model is used to reveal the basic system response. Next the new heart valve model developed in this paper is adopted and the corresponding simulation results are compared with those of the basic response, to reveal the advantage of the new heart

Table 1
Parameters for the heart

Part	Parameter	Value	Unit
Left heart	CQ_{ao}	350	ml/(s mmHg$^{0.5}$)
	CQ_{mi}	400	ml/(s mmHg$^{0.5}$)
	E_{lvs}	2.5	mmHg/ml
	E_{lvd}	0.1	mmHg/ml
	$P_{lv,0}$	1	mmHg
	$V_{lv,0}$	5	ml
	$E_{la,max}$	0.25	mmHg/ml
	$E_{la,min}$	0.15	mmHg/ml
	$P_{la,0}$	1	mmHg
	$V_{la,0}$	4	ml
Right heart	CQ_{po}	350	ml/(s mmHg$^{0.5}$)
	CQ_{ti}	400	ml/(s mmHg$^{0.5}$)
	E_{rvs}	1.15	mmHg/ml
	$E_{rv,d}$	0.1	mmHg/ml
	$P_{rv,0}$	1	mmHg
	$V_{rv,0}$	10	ml
	$E_{ra,max}$	0.25	mmHg/ml
	$E_{ra,min}$	0.15	mmHg/ml
	$P_{ra,0}$	1	mmHg
	$V_{ra,0}$	4	ml

Table 2
Parameters for the blood vessels

Branch	Parameter	Value	Unit
Systemic circulation	C_{sas}	0.08	ml/mmHg
	R_{sas}	0.003	mmHg s/ml
	L_{sas}	0.000062	mmHg s^2/ml
	C_{sat}	1.6	ml/mmHg
	R_{sat}	0.05	mmHg s/ml
	L_{sat}	0.0017	mmHg s^2/ml
	R_{sar}	0.5	mmHg s/ml
	R_{scp}	0.52	mmHg s/ml
	R_{svn}	0.075	mmHg s/ml
	C_{svn}	20.5	ml/mmHg
	C_{svc}	1.5	ml/mmHg
	V_{lv0}	800	ml
Pulmonary circulation	C_{pas}	0.18	ml/mmHg
	R_{pas}	0.002	mmHg s/ml
	L_{pas}	0.000052	mmHg s^2/ml
	C_{pat}	3.8	ml/mmHg
	R_{pat}	0.01	mmHg s/ml
	L_{pat}	0.0017	mmHg s^2/ml
	R_{par}	0.05	mmHg s/ml
	R_{pcp}	0.25	mmHg s/ml
	R_{pvn}	0.006	mmHg s/ml
	C_{pvn}	20.5	ml/mmHg
	C_{pvc}	1.5	ml/mmHg
	V_{rv0}	500	ml

Table 3
Parameters for variable valve opening model

Part	Parameter	Value	Unit
Systemic part	$K_{p,ao}$	5500	rad/(s^2 mmHg)
	$K_{f,ao}$	50	1/s
	$K_{b,ao}$	2	rad/(s m)
	$K_{v,ao}$	7	rad/(s m)
	$K_{p,mi}$	5500	m/(s^2 mmHg)
	$K_{f,mi}$	50	1/s
	$K_{b,mi}$	2	rad/(s m)
	$K_{v,mi}$	3.5	rad/(s m)
Pulmonary part	$K_{p,po}$	5500	rad/(s^2 mmHg)
	$K_{f,po}$	50	1/s
	$K_{b,po}$	2	rad/(s m)
	$K_{v,po}$	3.5	rad/(s m)
	$K_{p,ti}$	5500	rad/(s^2 mmHg)
	$K_{f,ti}$	50	1/s
	$K_{b,ti}$	2	rad/(s m)
	$K_{v,ti}$	3.5	rad/(s m)

Table 4
Valve opening angle

Parameter	Value	Unit
$\theta_{max,ao}$	75	degrees
$\theta_{min,ao}$	5	degrees
$\theta_{max,mi}$	75	degrees
$\theta_{min,mi}$	5	degrees
$\theta_{max,po}$	75	degrees
$\theta_{min,po}$	5	degrees
$\theta_{max,ti}$	75	degrees
$\theta_{min,ti}$	5	degrees
$\theta_{stenosis,mi}$	50	degrees
$\theta_{regurgation,ao}$	25	degrees

Table 5
Additional parameters

Parameter	Value	Unit
DT	0.0001	s
T	1	s
T_s	0.3	s
T_{pwb}	0.92	s
T_{pww}	0.09	s

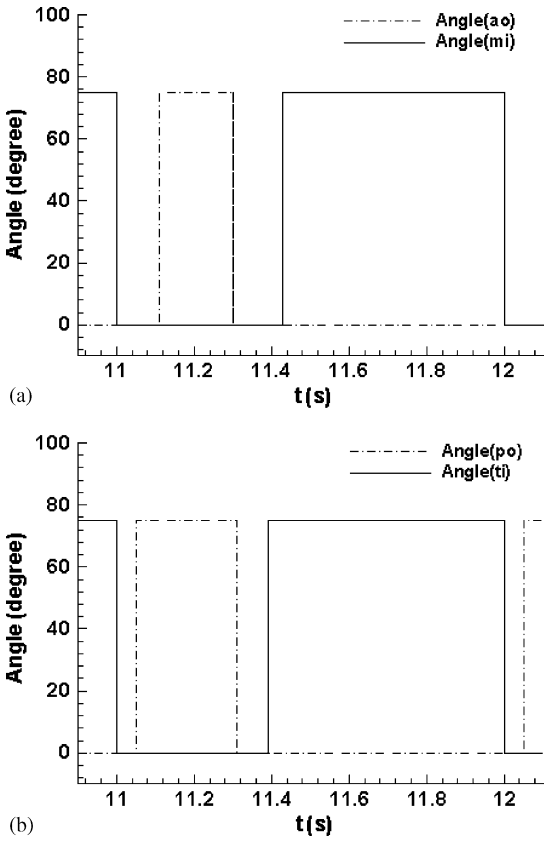

Fig. 4. Resultant change of heart valve leaflet angular position (opening) in the simplified model: (a) aortic and mitral valves; and (b) pulmonary and tricuspid valves.

valve model. Finally, the new system model is used to study cardiovascular response under two typical pathological conditions of heart valve diseases. For easy evaluation, the heart period is chosen to be 1 s the simulations. The dynamic system often reaches periodic solution after 6–7 heart cycles of calculation; thus the period from the 10th to 11th s in every case is selected as typical response for comparison of results.

In order to facilitate discussion of results, it is necessary to distinguish between normal regurgitant flow and the pathological regurgitant flow in the condition of valve incompetence. In previous research reverse blood flow in the valves in both of these two situations has been described with the common name of "regurgitant flow", thus leading to potential confusion of the normal and diseased conditions. In this paper, we call the reverse flow in the normal valve "reverse flow", and that in the situation of valve incompetence "regurgitant flow". In the derivation of the valve dynamics equations above, the unit for the valve opening angle is rad; in the following comparisons for valve opening angles under various situations, the unit is converted into degrees.

3.1. Response with the simplified model

First, the simulation is carried out using the simplified on–off heart valve model as described by Eq. (7). Fig. 4 shows the change of opening angles of the four heart valves simulated with traditional on–off valve model, and Fig. 5 shows the simulation results for pressure, flow rate, and volume changes in the systemic and pulmonary circulations with the simplified model.

From Fig. 4 it is observed that due to neglecting valve motion dynamics, the heart valves open and close rather abruptly, without showing the feature of three-stage motion pattern as described by Leyh et al. (1999). In Fig. 5, the simulation results for pressure, flow rate, and volume changes agree well with typical drawings of cardiovascular response shown in textbooks such as (Berne and Levy, 1981; Boron and Boulpaep, 2003; Guyton, 1986). The left ventricular pressure is in the range of 0−130 mmHg, and the aortic pressure changes between 90 and 130 mmHg. The peak systolic pressure is a little greater than the normal value of 120 mmHg. (Here the peak pressure is purposely elevated to about 130 mmHg in order that when the valve dynamics are considered, the pressure drop caused by normal reverse flow in the valves will bring the peak pressure back to the "normal" value of about 120 mmHg). Periodic peak flows exist in the mitral and aortic flows, with average flow-rate of about 5 l/min. The left ventricular volume

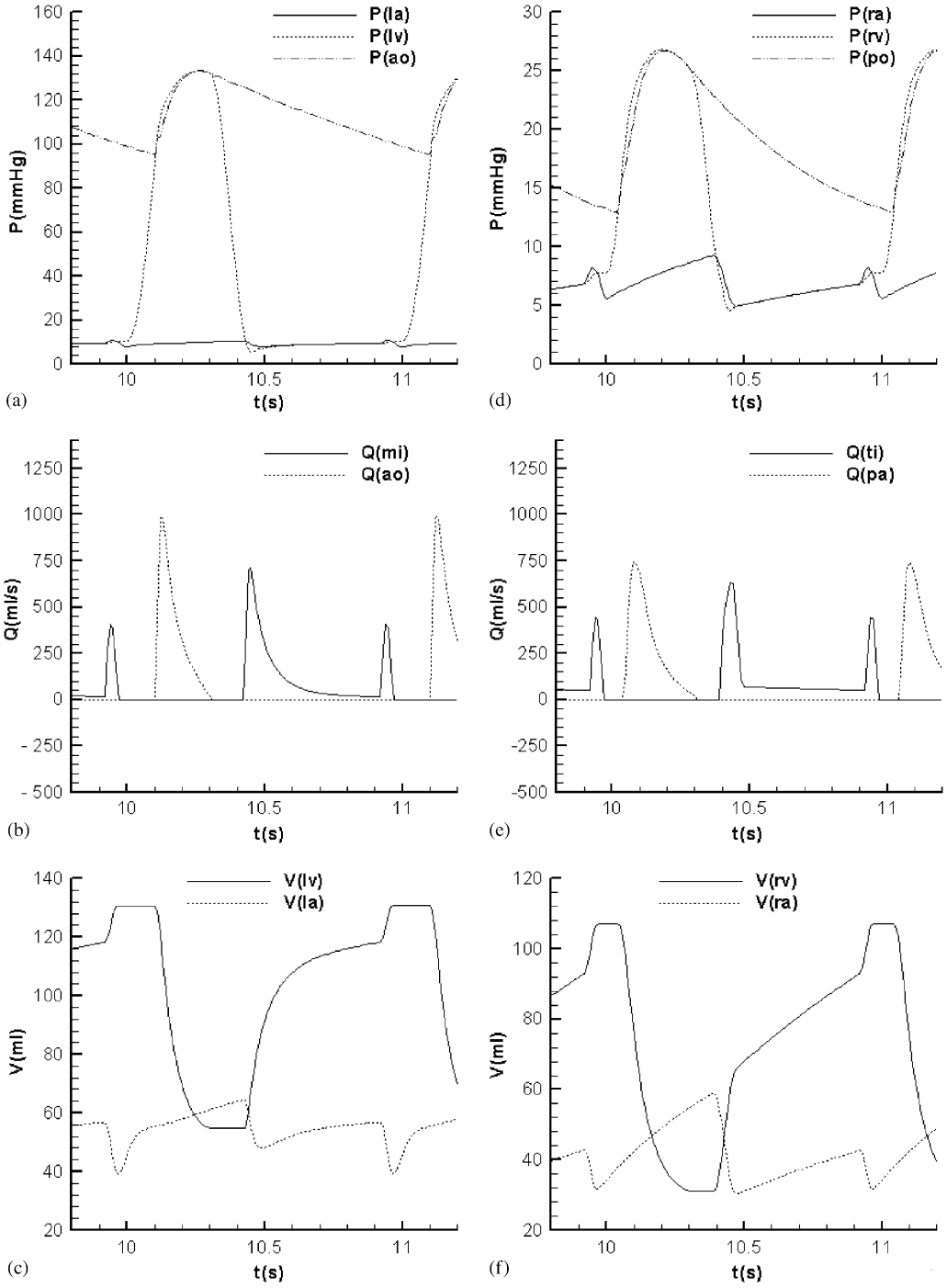

Fig. 5. System response with the basic cardiovascular system model: (a) pressure, left heart, (b) flow rate, left heart, (c) volume, left heart, (d) pressure, right heart, (e) flow rate, right heart, and (f) volume, right heart.

changes approximately between 50 and 120 ml, with a stroke volume of 70 ml. Because valve dynamics are not considered in this simplified model, certain important features such as the dicrotic notch in the aortic and pulmonary artery pressure, and normal reverse flow in the heart valves following valve closure, are missing from the simplified system response.

3.2. Response with modelling of normal heart valve dynamics

To study the effect of heart valve dynamics, Eq. (7) in the simplified model is replaced with Eq. (8). Parameter settings for heart valve dynamics are illustrated in Table 3. To specifically compare the

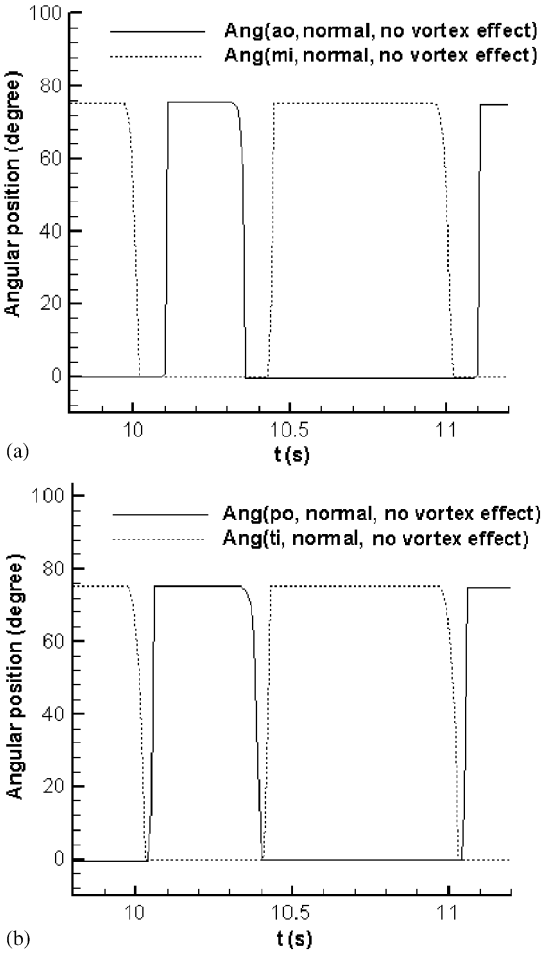

Fig. 6. Opening changes of normal heart valves with valve dynamics modelling and neglecting the vortex effect: (a) for mitral and aortic valves, (b) for tricuspid and pulmonary valves.

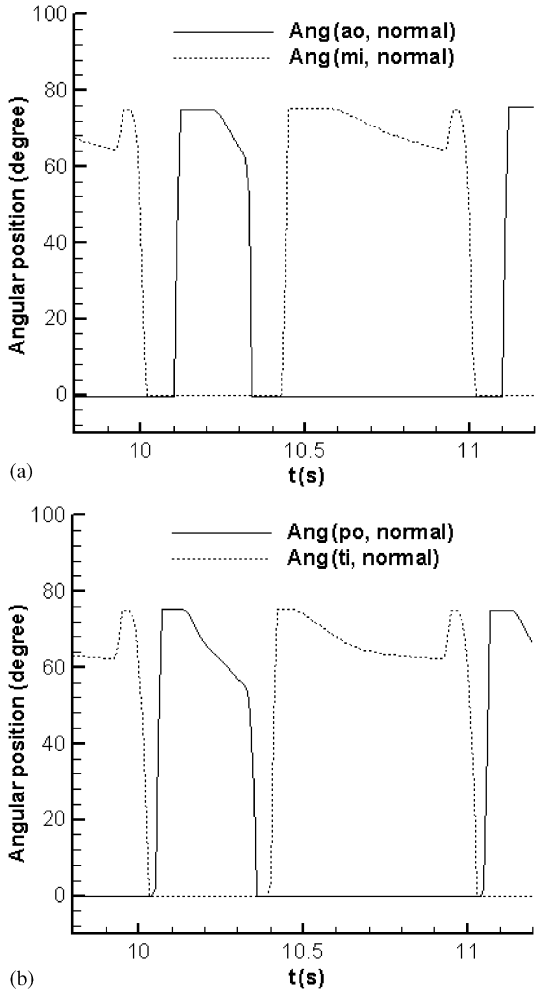

Fig. 7. Opening changes of normal heart valves with valve dynamics modelling and including the vortex effect: (a) for mitral and aortic valves, (b) for tricuspid and pulmonary valves.

influence of the vortex effect on valve motion, first the valve dynamics model is included, but the vortex effect is disabled by setting the corresponding coefficients $K_{v,ao}$, $K_{v,mi}$, $K_{v,po}$ and $K_{v,ti}$ to zero. Fig. 6 shows the corresponding results for the changes of valve leaflet angular position in the four valves. Next the vortex effect is enabled, and the corresponding valve motion is shown in Fig. 7. Fig. 8 illustrates the contribution of several factors including the pressure effect, frictional effect, velocity effect and the vortex effect, to the valve motion in one cycle.

In the valve opening sequences simulated with the simplified model shown in Fig. 4, the valves open and close abruptly, driven by the local pressure difference across the valves. In Fig. 6 the opening sequences become smoother with the introduction of the valve dynamics model. The valve opening and closing instances also change, and the effect is more pronounced in the response of the pulmonary and tricuspid valves. From Fig. 6, it is observed that the valve opening and closing processes take about 0.1 s. Comparing the valve motions in the right heart to that in the left heart, it is found that the pulmonary valve opens about 0.15 s earlier and closes about 0.1 s later than the aortic valve, and the tricuspid valve opens about 0.05 s earlier and closes about 0.05 s later than the mitral valve. This is closely related to the lower pressure range in the pulmonary loop and the slower pressure change rate in the right ventricle. The atrial pressures in the left and right heart are similar, thus the slower rise in pressure in the right ventricle induces the later closing of the tricuspid valve. The earlier opening of the tricuspid and pulmonary valves and the later closing of the pulmonary valve are the results of the combined actions of the lower pressure value in the pulmonary loop, and the slower rate of change of pressure in the right ventricle.

Fig. 6 gives improved descriptions of the valve motion sequence, however, the three-stage motion pattern as revealed by Leyh et al. (1999) is missing. To further test

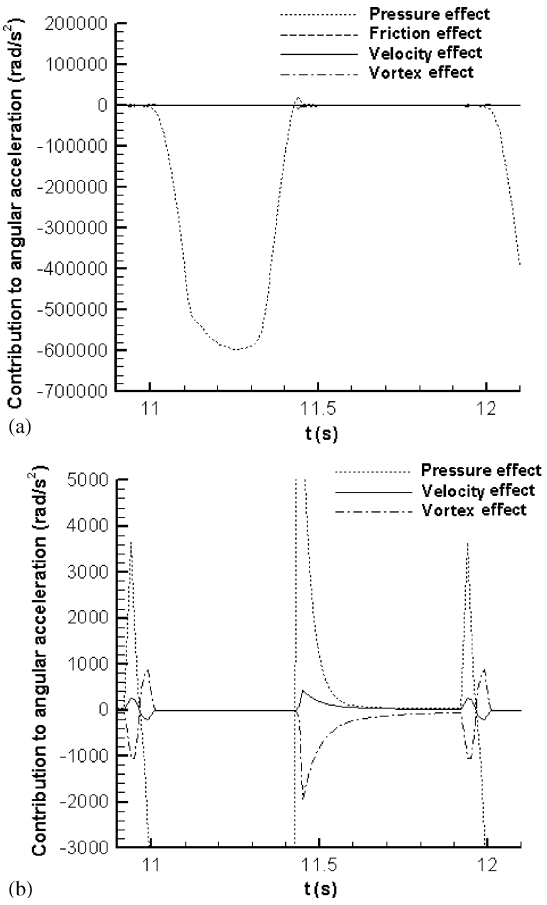

Fig. 8. Analysis of various factors in right hand side of Eq. 14 contributing to the valve motion, in rad/s^2: (a) in one cycle, (b) detailed view.

if the vortex effect plays a part in the three-stage valve motion pattern, the vortex effect is enabled in the valve dynamics model, which produces the results as shown in Fig. 7. In Fig. 7 it is observed that the three-stage motion pattern of fast opening, slow closing and fast closing, is clearly demonstrated in the valve motions. In the mitral and tricuspid valves, the leaflet regression motion to the fully open position is also present before the fast closing motion. This coincides with the illustrations presented in textbooks (Berne and Levy, 1981; Levick, 2003) for echo-cardiographic measurement of mitral valve dynamics.

To examine the underlying mechanism for the three-stage motion pattern in the mitral valve, the relative contribution of various factors in Eq. (14) in one heart cycle was evaluated, as illustrated in Fig. 8. Fig. 8(a) shows that in the systolic phase the pressure effect is the dominant factor for the mitral valve to fully close. In the early and late stages of the diastolic phase, as illustrated in Fig. 8(b), the pressure effect is still the most important factor for valve motion, while the vortex effect is the second most important factor. During diastole the timing (phase) of the velocity effect coincides with the pressure effect, but with a much smaller amplitude. Similarly in early systole, while the mitral and tricuspid valves are open and there is flow past the valves, the timing (phase) of the velocity effect coincides with the pressure effect, and is opposite to the vortex effect (during reverse flow), but the velocity and vortex effects have a much smaller amplitude than the pressure effect, which is dominant. The frictional effect is trivial compared with the above three factors, and is not shown in the figure for clarity of presentation.

Figs. 7 and 8(b) indicate that during the middle stage of the diastolic phase, the vortex effect is the most important factor to influence valve motion. It is this vortex effect that produces the slow closing motion in the three-stage valve motion pattern. The dominant pressure effect in the early stage of the diastolic phase causes the fast valve opening. In the end stage of the diastolic phase, due to atrial contraction the pressure effect becomes the dominant effect again; this produces the quick regression motion of the valve leaflet towards the fully open position. After that, the systolic phase begins and the greatly increased ventricular pressure reverses the direction of the pressure effect, and induces the fast closing stage of the valve motion. The three-stage motion pattern is also present in the aortic and pulmonary valves, but there is no regression motion before the fast valve closing process. This is because the regression motion is induced by atrial contraction, which affects only the mitral and tricuspid valves.

The above comparison of valve motion in different modelling cases suggests that valve dynamics modelling greatly improves the modelling accuracy, and the vortex effect plays an important role in the valve motion.

Fig. 9 compares the pressure, flow rate, and volume changes in the simplified model and the new model when valve dynamics are considered. Lines marked with a delta sign are the response when valve dynamics and the vortex effect are included in the model.

Figs. 9(a) and (d) compare the corresponding pressure responses. Generally the shape of the pressure waveforms remain the same with those of the simplified model, but the amplitudes of the waveforms decrease considerably. In the simplified model the peak ventricular pressure was purposely elevated to 130 mmHg, and now the decrease in pressure brings it back to the normal range of 120 mmHg. Modelling of valve dynamics reveals the reverse flows in the heart valves accompanying valve closure. The reverse flows decrease ventricular filling and the blood flow in the aorta and pulmonary artery. Thus it is observed that in the systolic phase, the peak pressure in the aorta and the left ventricle drop to 117.9 mmHg (from 126.4 mmHg in the simplified model), and in the pulmonary loop the peak pressure in the pulmonary artery and right ventricle drop from 26.8 to 26.1 mmHg. The pressure drop in the pulmonary loop is much smaller than that in the

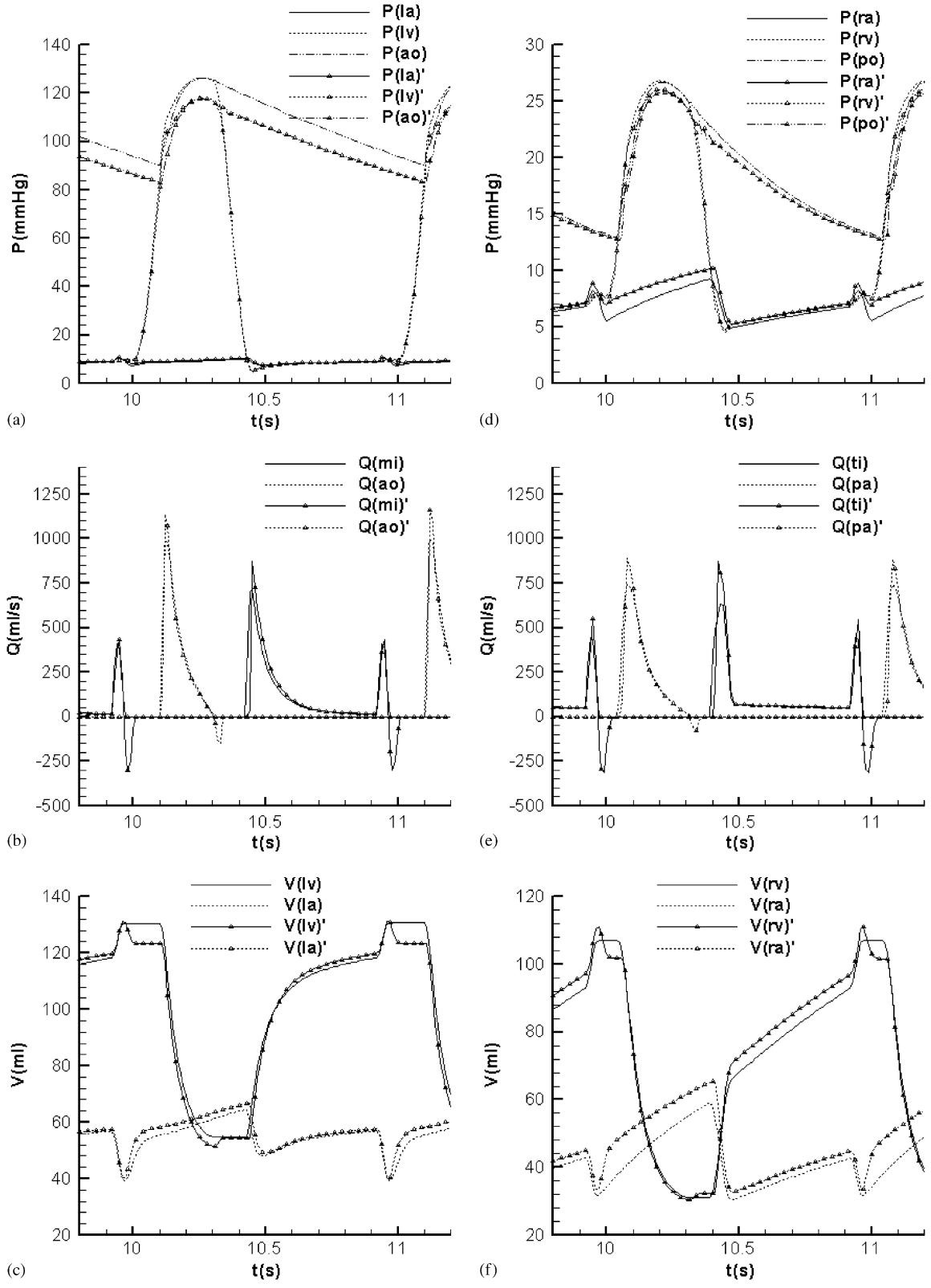

Fig. 9. System response with normal valve dynamics modelling including the vortex effect: (a) pressure, left heart, (b) flow rate, left heart, (c) volume, left heart, (d) pressure, right heart, (e) flow rate, right heart, (f) volume, right heart.

systemic loop in the systolic phase. Reverse flow in the aortic/pulmonary valve causes a pressure drop of about 8 mmHg in the aorta and a pressure drop of about 0.2−0.9 mmHg in the pulmonary artery in the diastolic phase, while it also induces negligible increase in the left and right ventricular pressures. The pressure drops in the right heart are much smaller than those in the left heart. This is due to the effect of the highly distensible blood vessels (and thus the greater compliance) in the pulmonary loop. Reverse flow to the atria also increases the atrial pressure throughout the heart cycle, which is more prominently exhibited in the pulmonary loop. Also it is observed that in the pressure waveforms of the aorta and the pulmonary artery, the closure of the aortic/pulmonary valve causes a local incisura called the "dicrotic notch". The dicrotic notch is the result of the combined action of valve closure, inertial effect of blood flow, and pulse wave reflection in the arteries. As the pulse wave reflection in the arteries can only be simulated through distributed parameter modelling or unsteady CFD computations, the dicrotic notch shown here is only due to the first two factors, thus the amplitude shown in the figures is smaller than that shown in textbooks.

Modelling of valve dynamics reveals the obvious feature of reverse flows in the flow-rate response in Figs. 9(b) and (e). In early diastole accompanying the closure of the aortic/pulmonary valves, there are reverse flows with amplitude of 134.3 ml/s in the aortic valve and 77.3 ml/s in the pulmonary valve. Similarly in early systole, accompanying the closure of the mitral/tricuspid valves, there are reverse flows with amplitude of 298.7 ml/s in the mitral valve and 306.9 ml/s in the tricuspid valve. Reverse flow through the mitral and tricuspid valves builds up more blood in the atria, and increases the preload, so that in early diastole the peak flow-rates corresponding to the E velocity peak increases from 702.9 to 826.0 ml/s in the mitral valve and from 631.7 to 861.0 ml/s in the tricuspid valve. Accompanying this, in early systole the peak aortic flow increases from 983.4 to 1128.3 ml/s, and the peak tricuspid flow also increases from 712.1 to 844.1 ml/s. In early diastolic phases regurgitant flow in the aortic and pulmonary valves slightly increase the ventricular pressure. Thus compared to that in the simplified model, the peak mitral/tricuspid flow corresponding to the E velocity peak occurs about 0.1 s later.

Compared with the results in the simplified model, reverse flow in the mitral and tricuspid valves increases the atrial volume, especially in the systolic phase, as illustrated in Figs. 9(c) and (f). This also increases atrial preload, thus naturally increasing the ventricular volume in the diastolic phase. In the systolic phase, however, the ventricles contract to a smaller volume due to the mitral/tricuspid reverse flow. In the early diastolic phase, the additional volume increase in the ventricles is due to aortic/pulmonary reverse flow. Similarly, mitral/tricuspid reverse flows cause additional volume drops in the ventricles, and volume increases in the atria in both the late diastolic and the early systolic phases.

3.3. Response with modelling of heart valve disease

Normal functioning of heart valves has a great influence on the cardiovascular physiology. Diseases in heart valves often occur in the systemic circulation, as regurgitation or stenosis in the mitral and aortic valves. The cases of mitral stenosis and aortic regurgitation are studied in this paper. In the following comparison, the lines marked with a delta sign are the response under diseased conditions, and those without the delta sign denote the response in the healthy condition.

3.3.1. Mitral stenosis

In the adult human the normal mitral valve orifice has a sectional area of 4−6 cm^2. However, flow across the valve remains unimpeded until the valve area is about half this, and not until the valve area is about one quarter of the normal value is valve stenosis regarded as critical (Timmis et al., 1997). To model the diseased condition of mitral stenosis, the maximum opening angle of the mitral valve in the developed model is changed from 75° to 50°, corresponding to 24% of the original valve area. The corresponding system response is illustrated in Figs. 10 and 11.

In Fig. 10 it is observed that, besides the reduction of the maximum opening angle of the mitral valve from 75° to 50°, the three-stage motion pattern in the mitral valve is not present. The mitral valve remains in the fully open position throughout the diastolic phase. The leaflet motion trajectory is similar to that in Fig. 6 for the situation when valve dynamics is considered, but the

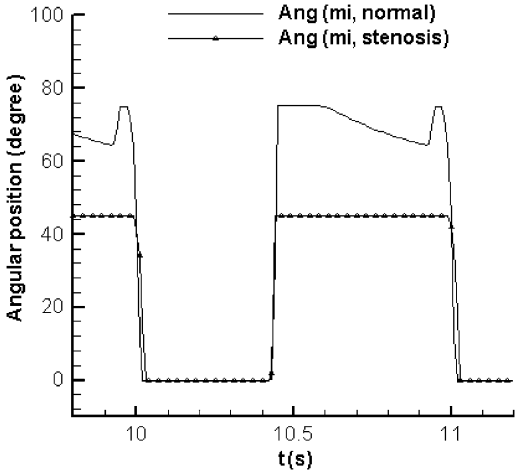

Fig. 10. Comparison of mitral valve motion between healthy condition and mitral stenosis.

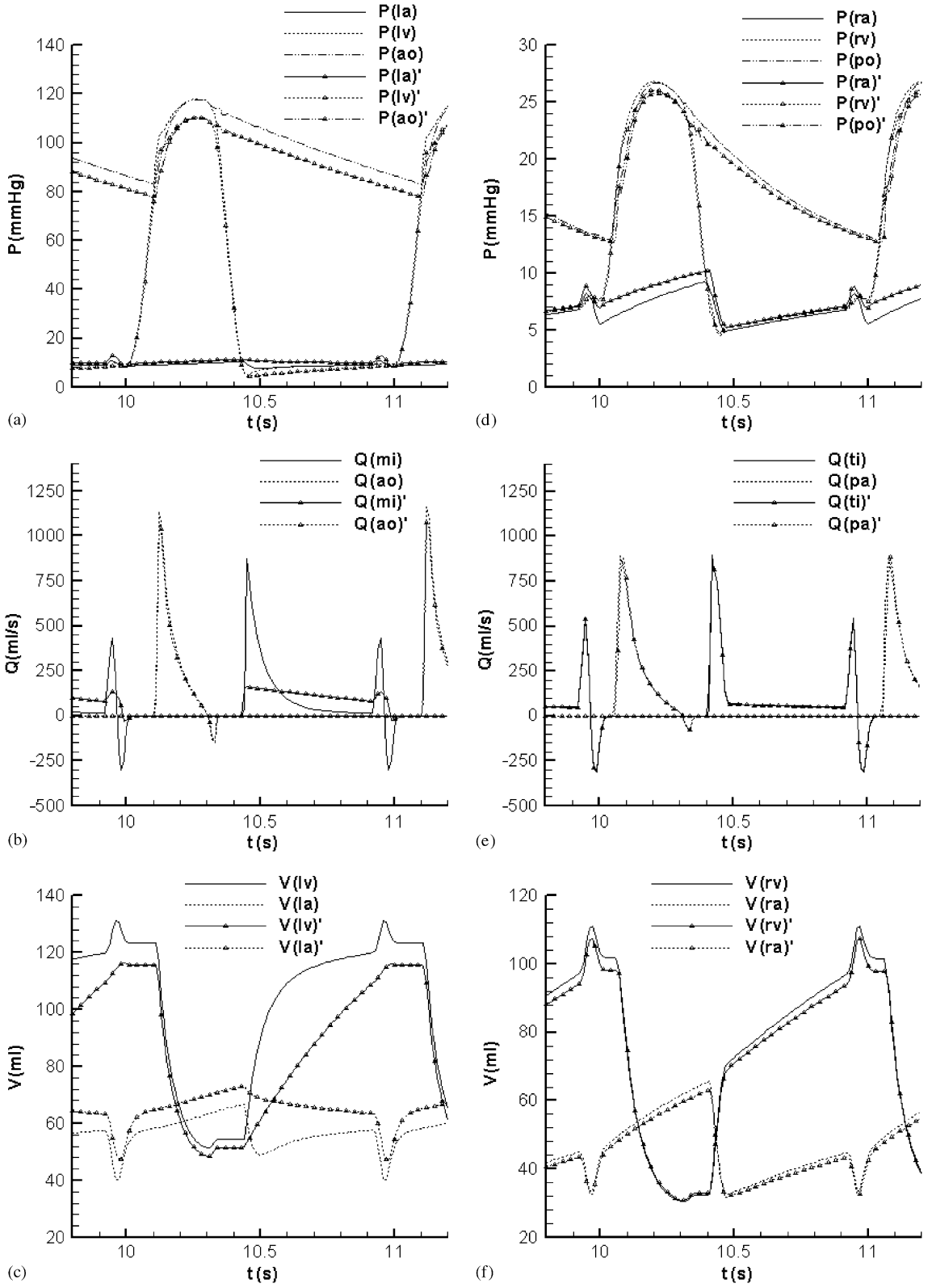

Fig. 11. System response with mitral stenosis: (a) pressure, left heart, (b) flow rate, left heart, (c) volume, left heart, (d) pressure, right heart, (e) flow rate, right heart, and (f) volume, right heart.

vortex effect is neglected. This is because mitral stenosis greatly impedes mitral flow, causing blood accumulation in the left atrium and elevating the left atrial pressure in diastole. The elevated left atrial pressure affects the mitral flow in diastole, making the pressure effect overshadow the vortex effect in diastole. Thus, the slow closing stage of valve motion in middle diastole and the regression motion of valve leaflet due to atrial contraction are not present in this condition.

In Figs. 11(a) and (d), it is observed that mitral stenosis causes a prominent pressure decrease in the left ventricle and the aorta, while pressure in the right ventricle and the pulmonary artery is slightly increased. In peak systole the left ventricular pressure is decreased from 117.8 to 110.4 mmHg, and in diastole it is decreased for about 0.8−2.1 mmHg. Throughout the heart cycle, the aortic pressure is decreased by about 6 mmHg, and the pressure in left atrium is elevated by about 0.9−3.1 mmHg. Accompanying the pressure increase in the left atrium, the pressures in the right ventricle and the pulmonary artery are also increased. In peak systole the pressure in the right ventricle and the pulmonary artery is increased by about 0.4 mmHg. In diastole the pulmonary artery pressure is increased by about 0.6−1.3 mmHg. Due to the decreased aortic pressure, the pressure in the right atrium is also slightly decreased all over the heart cycle.

Figs. 11(b) shows a prominent change in the mitral flow waveform. The original double peaks in the mitral flow corresponding to the E and A velocity disappear, and the flow becomes quite smoothed. In early diastole when the mitral valve is just open, the mitral flow has its maximum value of about 161.6 ml/s. During diastole, the mitral flow gradually decreases from the maximum value to the minimum value of about 80.9 ml/s. At end diastole, atrial contraction induces a local peak of about 132.7 ml/s in the mitral flow. Except this, there is no observable change in aortic flow. Flow in the right heart keeps the same as that in the normal heart, as shown in Fig. 11(e).

Figs. 11(c) shows that left ventricular volume is decreased by about 50 ml in the diastolic phase due to inadequate filling, and in the systolic phase it is also slightly reduced. This implies that the cardiac output is reduced. Due to mitral stenosis left atrial volume is prominently increased, which suggests atrial dilation. Because of the reduced cardiac output, volume in both right atrium and right ventricle is decreased, as shown in Figs. 11(c) and (f).

Mitral stenosis increases atrium load and may cause atrium dilatation, thus in the long term it will develop into atrial fibrillation, which heralds sclerosis. It also causes deficient preload to the left ventricle, thus greatly diminishing the transportation of oxygen and nutrients to the body. The simulated case is not a serious diseased condition. If mitral stenosis develops further, the fully open area of the mitral valve will decrease further. When the situation is so serious that the left atrial pressure rises above 18−20 mmHg, pulmonary edema and irreversible changes in pulmonary circulation will occur.

3.3.2. *Aortic regurgitation*

To simulate aortic regurgitation, in the valve dynamics calculation the minimum valve angle is changed from 0° to 25°, leaving a clearance for leakage flow across the valve during the diastolic phase. The corresponding valve motion is shown in Fig. 12, and the pressure, flow rate, and volume changes are illustrated in Fig. 13.

From Fig. 12 it is observed that generally the valve keeps the same trend of motion throughout the heart cycle, but the minimum opening angle is changed to 25°. The valve opening process begins 0.04 s earlier than in the normal case. The reason for the earlier valve opening process is that, aortic regurgitation decreases the aortic pressure, so that during systole it is easier for the ventricular pressure to exceed the aortic pressure. Aortic regurgitation mainly affects aortic flow in diastole, while the three-stage valve motion pattern in the aortic valve still exists in systole.

Figs. 13(a) and (d) show that in the systolic phase aortic and left ventricular pressures drop only slightly, by about 2.2 mmHg, while in diastolic phase there is a prominent decrease in the aortic pressure. At end diastole the aortic pressure drops from 86.5 mmHg in the normal case to 69.3 mmHg in the situation of aortic regurgitation, with a pressure drop of about 17 mmHg. This coincides with the clinical observation that aortic regurgitation greatly increases pressure pulsation in the aorta (Levick, 2003; Timmis et al., 1997). Pressure in the left atrium is slightly elevated throughout the heart cycle, due to reverse flow into the ventricle, which impedes the blood filling from atrium to the ventricle. In

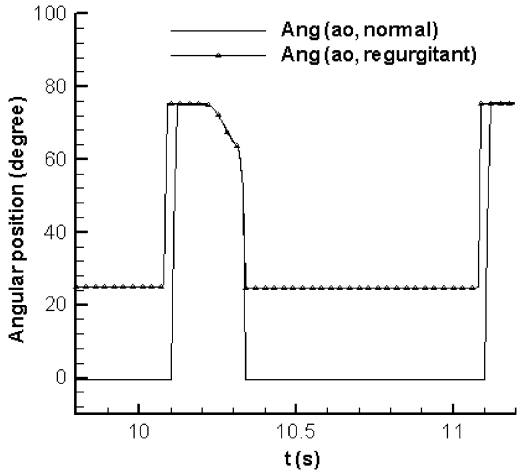

Fig. 12. Comparison of aortic valve motion between healthy condition and aortic regurgitation.

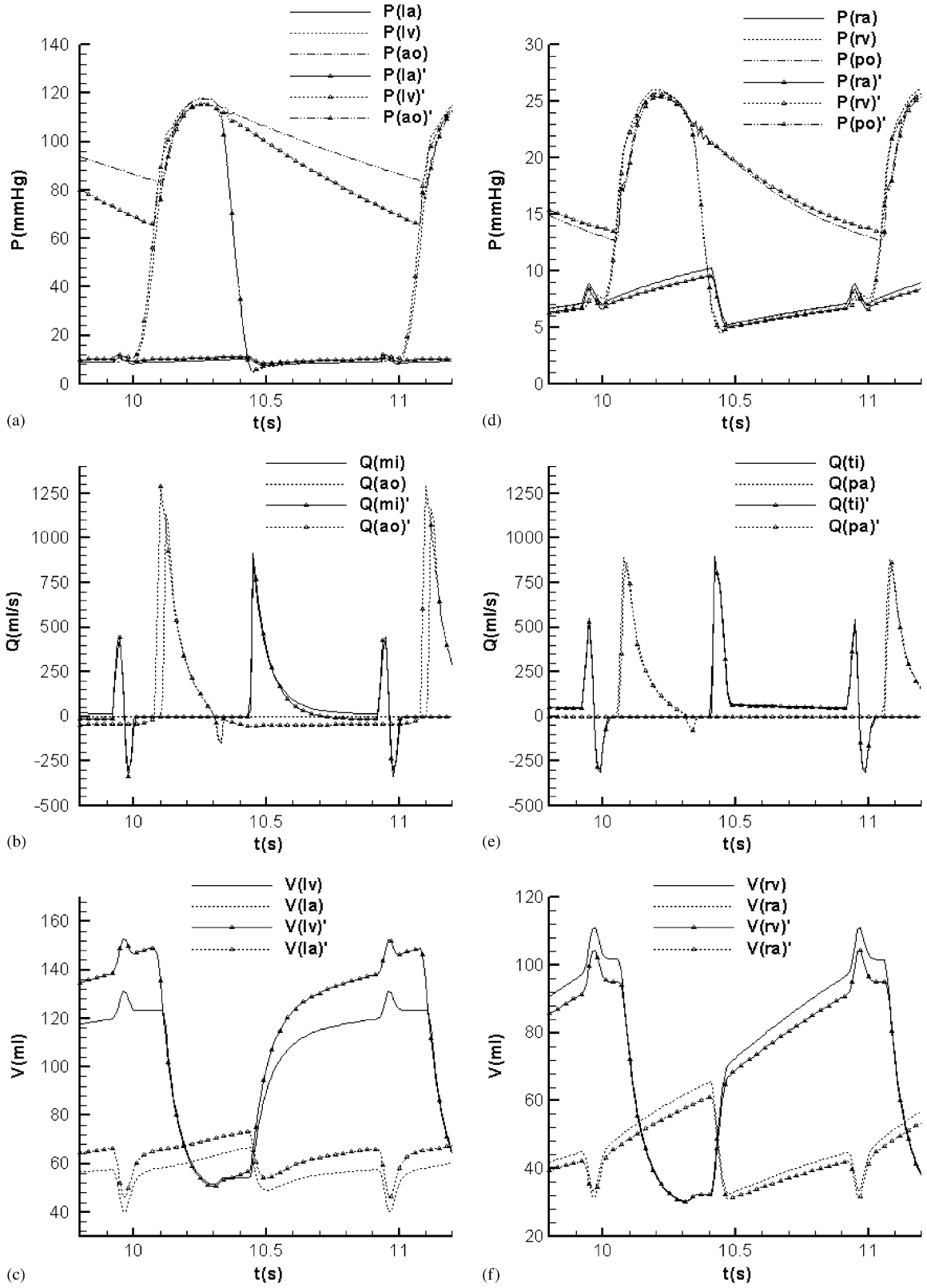

Fig. 13. System response with aortic regurgitation: (a) pressure, left heart, (b) flow rate, left heart, (c) volume, left heart, (d) pressure, right heart, (e) flow rate, right heart, and (f) volume, right heart.

the right heart, pressures in the pulmonary artery and the right ventricle are slightly elevated due to increased pressure in the left atrium, and the right atrial pressure is slightly decreased due to the decreased aortic pressure during diastole.

Figs. 13(b) and (e) show that during systole the peak aortic flow is increased from 1128.3 ml/s in normal case to 1270.2 ml/s in aortic regurgitation, and the aortic flow rises 0.04 s earlier than in the normal case. The reason for the increased peak aortic flow rate is that aortic regurgitation causes more blood to be accumulated in diastole, so that when the left ventricle contracts it induces increased flow rate. The reason for the earlier rise in aortic flow is the same as that for the earlier aortic valve opening. In diastole, aortic regurgitation presents itself as a persistent aortic reverse flow from the aorta to the left ventricle, with an amplitude of about 47.9 ml/s. This aortic reverse flow slightly elevates the left ventricular pressure, thus the mitral flow is slightly decreased in middle diastole. In the right heart there is no observable flow rate change in the tricuspid and pulmonary valves.

Figs. 13(c) and (f) show that in the left heart, aortic regurgitation greatly increases the left ventricular volume. At end diastole, the left ventricular volume is increased from 123.4 ml in the normal case to 149.0 ml in the case with aortic regurgitation. In systole the left ventricular volume keeps the same value as in the normal situation. The increased volume difference in the left ventricle corresponds to more flow across the aortic valve during the heart cycle, but does not suggest an increased cardiac output, as the reverse flow across the aortic valve negates the increased output. Thus, aortic regurgitation volume loads the heart, and in the long term it will cause ventricular dilatation and ventricular hypertrophy (Timmis et al., 1997). Throughout the heart cycle left atrial volume is also prominently increased. Thus, aortic regurgitation also has negative impacts on the left atrial function and in the long term it will cause atrial fibrillation. In the right heart the volumes of both the ventricle and the atrium are decreased, corresponding to diminished systemic function.

4. Discussion and conclusion

This paper presents a new model for the human cardiovascular system which includes an innovative model for heart valve dynamics. The new valve model considers the pressure, flow, tissue friction, and vortex effects of blood flow acting around the heart valves. The resultant model illustrates how each one of these effects influences the three stages of valve motion patterns in healthy and diseased conditions.

In deriving the valve dynamics equation, the pressure flow-rate relation in the valve is described with the orifice equation, and the valve opening change is decided from the valve leaflet opening angle. Calculation of leaflet opening angle is directly based on the governing differential equation for leaflet motion, by considering the various effects acting on the valve including the pressure difference, the fluid motion, neighboring tissue friction, vortex effect etc. This modelling process has clear physical meaning and is straightforward. This detailed modelling of heart valve dynamics helps to reveal the reverse flow phenomena in the valves during valve closing, and also contributes to the explanation of the dicrotic notch in the aortic and pulmonary valves. In most previous research, the heart valves are modelled as a combination of a resistance and a diode. This simplification is justified in situations when the research is focused on other aspects of cardiovascular dynamics such as under neuro-reflex regulation, interaction of cardiac dynamics, and respiration dynamics, etc. At the same time the simplification also results in the inability of previous models to accurately describe important physiological and pathological changes in the heart valves such as: reverse flow upon valve closure; and regurgitant flow in valve incompetence. These important changes have critical meaning in physiological study and clinical practice. Some researchers considered valve behavior, such as the reverse flow upon valve closure and the variable valve resistance during valve opening and closing processes, but the valve motion in their models is prescribed based on experience, and the physical mechanism governing valve dynamics was not analyzed. Thus, these models lack proper justification. As a comparison, the current heart valve model avoids such shortcomings by directly analyzing the various factors that affect the valve dynamics, thus revealing the underlying physical essence of valve motion by considering the blood–valve interaction effect. Also as a compromise between simplicity in modelling and elaboration of the complex coupling between blood flow and valve motion, the current valve dynamics modelling reaches a balance between accuracy and economy. The simulated results are then analyzed by comparing with the situation of neglecting valve dynamics modelling. Through this modelling, the valve motion details were accurately revealed, such as duration of the opening and closing process and timing of motion among the four valves in a heart cycle. The comparison validates the advantage of the proposed new valve model.

The vortex effect has an important influence on valve motion dynamics, as indicated by previous researchers and through clinical and experimental investigations. Despite the various CFD studies, successful numerical simulation of this effect in valve dynamics has not been achieved due to the difficulty in accurately describing the blood–leaflet interaction effect and the expensive computing resources required. Simplified modelling of this effect on the valve dynamics has not been previously

attempted. Based on the results of previous clinical and experimental observations, the current paper proposes a concentrated parameter description of the vortex effect on valve motion dynamics. The proposed description is incorporated in the new valve dynamics model. This modelling shows clearly the typical three-stage motion pattern of fast opening, slow closing and fast closing in valve motion, as revealed by previous clinical observations. A realistic description of regression motion of leaflet in the mitral/tricuspid valve near the end of diastole, as recorded by clinical echo-cardiography study, is also vividly revealed by combining the new valve model with the model for atrial contraction.

The proposed numerical model is used to study two typical pathological cases of mitral stenosis and aortic regurgitation. Analysis of detailed valve motion dynamics, together with the pressure, flow-rate, and volume response in these two cases, successfully duplicate the pathological changes in the corresponding diseased conditions, thus further validating the current model. All these effects are easily simulated with the current numerical model, while not all of these aspects are easily obtained through clinical observation. The current numerical model has great potential in assisting cardiovascular physiology studies and clinical cardiac diagnoses.

References

Bellhouse, B.J., 1972. The fluid mechanics of heart valves. In: Bergel, D.H. (Ed.), Cardiovascular Fluid Dynamics, vol. 1, (Chapter 8). Academic Press, New York.

Berne, R.M., Levy, M.N., 1981. Cardiovascular Physiology, fourth ed. The C.V. Mosby Company, St. Louis, MO.

Bluestein, D., Einav, S., 1994. Transition to turbulence in pulsatile flow through heart valve—a modified stability approach. Journal of Biomechanical Engineering 122, 125–134.

Boron, W.F., Boulpaep, E.L., 2003. Medical Physiology: A Cellular and Molecular Approach. Saunders, London.

Brucker, C.H., 1997. Dual-camera dpiv for flow studies past artificial heart valves, experiments in fluids. Experiments in Fluids 22, 496–506.

Chambers, J., Ely, L., 1998. Early postoperative echocardiographic hemodynamic performance of the on-x prosthetic heart valve: a multicenter study. Journal of Heart Valve Disease 7, 569–573.

Chew, Y.T., Low, H.T., Lee, C.N., Kwa, S.S., 1993. Laser anemometry measurements of steady flow past aortic valve prostheses. Journal of Biomechanical Engineering 115, 290–298.

Drzewiecki, G., Wang, J.-J., Li John, K.-J., Kedem, J., Weiss, H., 1996. Modeling of mechanical dysfunction in regional stunned myocardium of the left ventricle. IEEE Transaction on Biomedical Engineering 43 (12), 1151–1163.

Durand, L., Garcia, D., Sakr, F., Save, H., Cimon, R., Pilbarot, P., Fenster, A., Dumesnil, J., 1999. A new flow model for doppler ultrasound study of prosthetic heart valves. Journal of Heart Valve Disease 8 (1), 85–95.

Fung, Y.C., 1984. Biodynamics: Circulation. Springer, Berlin.

Grigioni, M., Daniele, C., D'Avenio, G., Barbaro, V., 2000. Hemodynamic performance of small-sized bileaflet valves: pressure drop and laser doppler anemometry study comparison of three prostheses. Artificial Organs 24 (12), 959–965.

Guyton, A.C., 1986. Textbook of Medical Physiology. WB Saunders, Philadelphia, PA.

De Hart, J., Paters, G.W.M., Schreurs, P.J.G., Baaijens, F.P.T., 2000. A two-dimensional fluid-structure model of the aortic valve. Journal of Biomechanics 33, 1079–1088.

De Hart, J., Paters, G.W.M., Schreurs, P.J.G., Baaijens, F.P.T., 2003a. A three-dimensional computational analysis of fluid-structure interaction in the aortic valve. Journal of Biomechanics 36, 103–112.

De Hart, J., Baaijens, F.P.T., Paters, G.W.M., Schreurs, P.J.G., 2003b. A computational fluid-structure interaction analysis of a fiber-reinforced stentless aortic valve. Journal of Biomechanics 36, 699–712.

Healy, T.M., Fontaine, A.A., Ellis, J.T., Walton, S.P., Yoganathan, A.P., 1998. Visualization of the hinge flow in a 5:1 scaled model of the medtronic parallel bileaflet heart valve prosthesis. Experiments in Fluids 25, 512–518.

Heldt, T., Shim, E.B., Kamm, R.D., Mark, R.G., 2002. Computational modeling of cardiovascular response to orthostatic stress. Journal of Applied Physiology 92, 1239–1254.

Huang, Z.J., Merkle, C.L., Abdallah, S., Tabell, J.M., 1994. Numerical simulation of unsteady laminar flow through a tilting disk heart valve: prediction of vortex shedding. Journal of Biomechanics 27 (4), 391–402.

Kiris, C., Kwak, D., Rogers, S., Chang, I-D., 1997. Computational approach for probing the flow through artificial heart devices. Journal of Biomechanics 119, 452–460.

Lai, Y.G., Chandran, K.B., Lemmon, J., 2002. A numerical simulation of mechanical heart valve closure fluid dynamics. Journal of Biomechanics 35, 881–892.

Levick, J.R., 2003. An introduction to Cardiovascular Physiology, fourth ed. Arnold, London.

Leyh, R.G., Schmidtke, C., Sievers, H.-H., Yacoub, M.H., 1999. Opening and closing characteristics of the aortic valve after different types of valve-preserving surgery. Circulation 100, 2153–2160.

Lim, W.L., Chew, Y.T., Chew, T.C., Low, H.T., 1998. Steady flow dynamics of prosthetic aortic heart valves: a comparative evaluation with piv techniques. Journal of Biomechanics 31, 411–421.

Lu, K., Clark Jr., J.W., GhorBel, F.H., Ware, D.L., Bidani, A., 2001. A human cardiopulmonary system model applied to the analysis of the valsalva maneuver. American Journal of Physiology (Heart Circulation of Physiology) 281, H2661–H2679.

Makhijani, V.B., Siegel Jr., J.M., Hwang, N.H.C., 1996a. Numerical study of squeeze-flow in tilting disc mechanical heart valves. Journal of Heart Valve Disease 5, 97–103.

Makhijani, V.B., Siegel, J.M. Jr., Singhal, A.K., 1996b. Coupled fluid-structure analysis of bi-leaflet mitral mechanical heart valve dynamics. Advances in Bioengineering ASME BED-33.

Makhijani, V.B., Yang, H.Q., Dionne, P.J., Thubrikar, M.J., 1997. Three-dimensional coupled fluid-structure simulation of pericardial bio-prosthetic aortic valve function. ASAIO Journal 48, M387–M392.

Pennati, G., Bellotti, M., Fumerco, R., 1997. Mathematical modelling of the human foetal cardiovascular system based on doppler ultrasound data. Medical Engineering & Physics 19 (4), 327–335.

Shi, Y.B., Zhao, Y., Yeo, J.H., Hwang, N.H.C., 2003. Numerical simulation of opening process in a bileaflet mechanical heart valve under pulsatile flow condition. Journal of Heart Valve Disease 12, 245–256.

Shi, Y., Yeo, T.J.H., Zhao, Y., 2004. Numerical simulation of a systemic flow test rig. ASAIO Journal 50, 54–64.

Shim, E.B., Chang, K.S., 1997. Numerical analysis of three-dimensional Björk–Shiley valvular flow in an aorta. Journal of Biomechanical Engineering 119, 45–51.

Subramanian Mu, H., Kadambi, J.R., Wernet, M.P., Brendzel, A.M., Harasaki, H., 2000. Particle image velocimetry investigation of intravalvular flow fields of a bileaflet mechanical heart valve in a pulsatile flow. Journal of Heart Valve Disease 9 (5), 721–731.

Suga, H., Sagawa, K., Shoukas, A.A., 1973. Load independence of the instantaneous pressure–volume ratio of the canine left ventricle and effects of epinephrine and heart rate on the ratio. Circulation Research XXXII (314–322).

Thomas, J.D., Zhou, J., Greenberg, N., Bibawy, G., McCarthy, P.M., VanDervoort, P.M., 1997. Physical and physiological determinants of pulmonary venous flow: numerical analysis. American Journal of Physiology(Heart Circulation and Physiology) 272 (41), H2453–H2465.

Timmis, A.D., Nathan, A.W., Sullivan, I.D., 1997. Essential Cardiology, third ed. Blackwell Science, Oxford.

Underwood, F.N. Jr., 1975. A numerical study of the steady, axisymmetric flow through a disk type prosthetic heart valve. Ph.D. Thesis, Graduate school of University of Notre Dame.

Ursino, M., 1998. Interaction between carotid baroregulation and the pulsating heart: a mathematical model. American Journal of Physiology(Heart Circulation and Physiology) 275 (44), H1733–H1747.

Ursino, M., 1999. A mathematical model of the carotid baroregulation in pulsating conditions. IEEE Transaction on Biomedical Engineering 46 (4), 382–392.

Vollkron, M., Shima, H., Huber, L., Wieselthaler, G., 2002. Interaction of the cardiovascular system with an implanted rotary assist device: simulation study with a refined computer model. Artificial Organs 26 (4), 349–359.

Werner, J., Böhringer, D., Hexamer, M., 2002. Simulation and prediction of cardiotherapeutical phenomena from a pulsatile model coupled to the Guyton circulation model. IEEE Transaction on Biomedical Engineering 49 (5), 430–439.

West, J.B., 1990. Best and Taylor's Physiological Basis of Medical Practice, twelfth ed. Williams & Wilkins, Baltimore, MD.

Yacoub, M.H., Kilner, P.J., Birks, E.J., Misfeldn, M., 1996. The aortic outflow and root: a tale of dynamism and crosstalk. Annals of Thoracic Surgery 68, S37–S43.

Žáček, M., Krause, E., 1996. Numerical simulation of the blood flow in the human cardiovascular system. Journal of Biomechanics 19 (1), 13–20.